Structural and magnetic properties of $La_{0.67}(Ba_xCa_{1-x})_{0.33}MnO_3$ perovskites $(0 \leqslant x \leqslant 1)$

N. Moutis, I. Panagiotopoulos, M. Pissas, and D. Niarchos
Institute of Materials Science National Centre for Scientific Research, Demokritos, 153 10 Aghia Paraskevi, Athens, Greece
(Received 28 May 1998; revised manuscript received 28 July 1998)

The magnetic critical behavior in the series $La_{0.67}(Ba_xCa_{1-x})_{0.33}MnO_3$ $(0 \leqslant x \leqslant 1)$ of manganese perovskites is studied by means of dc magnetic measurements. In this series the Mn^{4+}/Mn^{3+} ratio is kept constant while Ca ions are substituted by the larger Ba ions resulting in structural changes accompanied by an increase of the transition temperature from 265 to 340 K. Samples with $x \leqslant 0.4$ crystallize in the orthorhombic $Pnma$ space group whereas samples with $x \geqslant 0.5$ in the rhombohedral $R\bar{3}c$ space group. Arrott and scaling plots show that only in samples with $x \geqslant 0.25$ the magnetic properties follow the behavior expected for a conventional second-order ferromagnetic transition. The values of critical exponents (β, γ) are between those predicted for a three-dimensional Heisenberg model and those predicted by mean field theory. [S0163-1829(99)04501-4]

I. INTRODUCTION

The correlation of magnetism and conductivity in mixed valence manganese perovskites was originally explained within the double-exchange model.[1] Recent theoretical work indicated the need to consider a strong electron-lattice coupling, due to dynamic Jahn-Teller distortions of the lattice, in order to account for the colossal magnetoresistance effect that these materials exhibit.[2,3] In the case of strong electron-phonon coupling the ferromagnetic, metallic state is destroyed above T_c due to polaron formation that leads to localization of the conduction band electrons. Substantial pressure effects on the T_c and electrical resistivity have been observed by Neumeier *et al.*[4] on $La_{2/3}Ca_{1/3}MnO_3$ and these results are interpreted in the framework of the double-exchange interaction involving conduction via magnetic polarons. Evidence of a nonconventional magnetic transition was found by Lynn *et al.*,[5] by neutron scattering studies on $La_{2/3}Ca_{1/3}MnO_3$ polycrystalline samples that revealed a strong quesielastic component dominating the spectrum as the transition temperature is approached. As this study indicated the transition is driven by spin diffusion rather than thermal population of conventional spin waves, while the presence of irreversibility also proves that the transition is not a conventional second order ferromagnetic to paramagnetic one. Muon-spin relaxation experiments also suggested unusual relaxational dynamics that could be attributed to polaron formation.[6] Furthermore, comparison of thermal expansion, magnetic susceptibility measurements and small angle neutron experiments[7] showed that the presence of small ferromagnetic clusters above T_c is related to an anomalous volume lattice distortion providing evidence for magnetic polaron formation. A comparative study of perovskite manganites with different T_c ($Nd_{0.7}Sr_{0.3}MnO_3$ with $T_c = 197.9$ K and $Pr_{0.63}Sr_{0.37}MnO_3$ with $T_c = 300.9$ K) showed that the spin dynamical behavior can be drastically different around T_c.[8] The ferromagnetic transition of the low T_c samples is characterized by the formation of spin clusters whereas the high T_c sample shows a more conventional behavior. The T_c of perovskite manganites of the type $AMnO_3$ can be continuously varied by various substitutions. A large number of studies has focused recently on the effect of the mean A-site ionic radius on the magnetic and magnetotransport properties.[9–21] When the doping of the A site with bivalent ions is kept constant, the main effect of the A-site substitutions is to change the structural parameters such as Mn-O-Mn bond angles and Mn-O bond lengths allowing the study of the effect of the structure on the magnetic properties. An increasing deviation from the typical Curie-Weiss behavior has also been observed in the $(Nd_{1-y}Sm_y)_{1/2}Sr_{1/2}MnO_3$ series as the T_C is lowered with y.[17] Apart from the direct effect of A-site cation substitutions on the structural parameters the effects of the variance $\sigma_A = \sqrt{\langle r_A^2 \rangle - \langle r_A \rangle^2}$ of the r_A distribution[22,24] and the electronegativity of the substituted ion[25] on the magnetotransport properties have been also considered.

In this work we present a study of the structural and magnetic properties of $La_{0.67}(Ba_xCa_{1-x})_{0.33}MnO_3$ ($x = 0$, 0.15, 0.25, 0.3, 0.4, 0.5, 0.75, 1) perovskites. The doping with Mn^{4+} is kept constant to a value of 1/3 for which ferromagnetic interactions are dominant[26] whereas by a systematic substitution of the Ca ion by Ba which has a larger ionic radius[27] the range of compositions between the $La_{0.67}Ca_{0.33}MnO_3$ and $La_{0.67}Ba_{0.33}MnO_3$ is covered.

II. EXPERIMENT

$La_{0.67}(Ba_xCa_{1-x})_{0.33}MnO_3$ samples were prepared by standard solid state reaction from stoichiometric amounts of La_2O_3, $CaCO_3$, $BaCO_3$ and MnO_2 powders, sintered at 1325–1400 °C, depending on the composition, for 5 days with two intermediate grindings. X-ray powder diffraction (XRD) data were collected with a Siemens D500 diffractometer using Cu $K\alpha$ radiation and a secondary graphite monochromator from 20° to 90° with a step size of 0.03° in 2θ mode and counting rate of 10 sec/step. dc magnetization measurements were performed in a superconducting quantum interference device (SQUID) magnetometer (Quantum Design). Magnetization isotherms at various temperatures around the critical region, have been measured in applied fields up to 10 kOe at temperature steps 1 K apart.

III. STRUCTURAL CHARACTERIZATION

The refinement of the XRD patterns was carried out by the BBWS-9006 Rietveld program.[28] All the samples were

TABLE I. Summary $La_{0.67}(Ba_xCa_{1-x})_{0.33}MnO_3$ samples. The reported unit cell constants of the $R\bar{3}c$ space group are in the hexagonal axes setting. Numbers in the parenthesis are errors of the last significant digit

x	0.00	0.15	0.25	0.30	0.40
			$Pnma$		
$\langle r_A \rangle$ (Å)	1.204	1.219	1.228	1.233	1.243
a(Å)	5.4562(2)	5.4647(2)	5.4720(2)	5.4728(1)	5.4787(1)
b(Å)	7.7092(2)	7.7195(2)	7.7283(3)	7.7266(2)	7.7351(1)
c(Å)	5.4697(1)	5.4878(1)	5.5014(2)	5.5062(1)	5.5114(1)
V_{cell}/Mn (Å^3)	57.52	57.88	58.16	58.21	58.43
T_c (K)	265	275	278	293	302
			$R\bar{3}c$		
x	0.50	0.75	1.00		
$\langle r_A \rangle$ (Å)	1.252	1.277	1.301		
a(Å)	5.5088(3)	5.5215(3)	5.5324(2)		
b(Å)	5.5088(3)	5.5215(3)	5.5324(2)		
c(Å)	13.3905(2)	13.4491(3)	13.5104(2)		
V_{cell}/Mn (Å^3)	58.65	59.2	59.7		
T_c (K)	308	323	340		

found to be single phase. Detailed results of the refinement procedure will be reported elsewhere.[23] Here we report only lattice constants (Table I) along with the unit cell volume normalized per Mn atom to allow comparison between samples described by different space groups. For all the samples with $x \leqslant 0.4$ the structure can be described by an orthorhombic unit cell (space group $Pnma$). Samples with $x \geqslant 0.5$ cannot be consistently indexed by an orthorhombic unit cell and are described by an rhombohedral unit cell (space group $R\bar{3}c$). A systematic increase of the cell volume from 57.5 to 59.7 Å^3 per Mn atom is observed as Ca ions are substituted by the larger Ba ions. Using the effective ionic radii given by Shannon[27] and following the convention of taking the ninefold coordination values,[15] we have calculated mean ionic radii ($\langle r_A \rangle$) which are also listed in Table I. According to our analysis the critical value of $\langle r_A \rangle$ for the orthorhombic to rhombohedral transition lies between 1.24 and 1.25 Å in agreement with Radaelli *et al.* (Ref. 15). The ionic radii of the constituent ions are known to determine the kind and degree of distortion of the simple cubic perovskite structure.[29,30] In order to relieve the stresses in the bonds, the MnO_6 octahedra are cooperatively rotated resulting in lower symmetry structures as the orthorhombic ($Pnma$) or the rhombohedral ($R\bar{3}c$) considered here. In this series of samples, where the Mn^{4+}/Mn^{3+} ratio and consequently the Mn site mean ionic radius is kept constant, the increase of the A-site mean ionic radius from 1.2 to 1.3 Å is expected to lead to structures closer to that of the ideal simple cubic perovskite with average Mn-O-Mn bond angle increased towards values closer to 180°.

IV. MAGNETIC MEASUREMENTS

Figure 1 shows the magnetization as a function of temperature (M vs T) measured in an applied field $H=1$ kOe. The transition temperature, determined from the inflection point of the M vs T curves, is found to increase from 265 K for the $La_{0.67}Ca_{0.33}MnO_3$ ($x=0$) sample to 340 K for the $La_{0.67}Ba_{0.33}MnO_3$ ($x=1$) sample. The values of the T_c are listed in the last row of Table I. The ferromagnetic behavior at temperatures around the T_c can be studied with the use of M^2 vs H/M plots (Arrott plots).[31,32] Near the critical temperature of a second order transition, the free energy F can be expanded in terms of the order parameter M in the following way:

$$F = F_0 - HM + aM^2 + bM^4 + \cdots . \tag{1}$$

DeGennes[33] has worked out a molecular field approximation for the case of mixed valence manganites and has calculated the coefficients a and b involved in Eq. (1). By minimizing F we can see that M^2 and H/M are related by

$$H/M = 2a + 4bM^2. \tag{2}$$

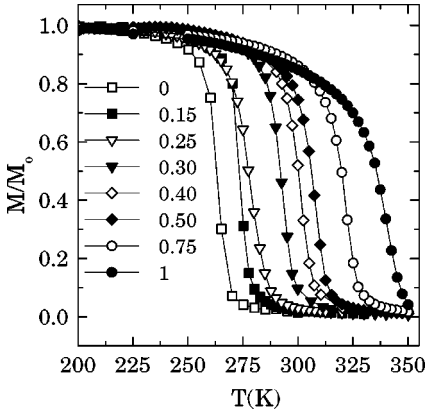

FIG. 1. Normalized magnetization vs temperature measured at an applied field of 1 kOe for the $La_{0.67}(Ba_xCa_{1-x})_{0.33}MnO_3$ series of samples.

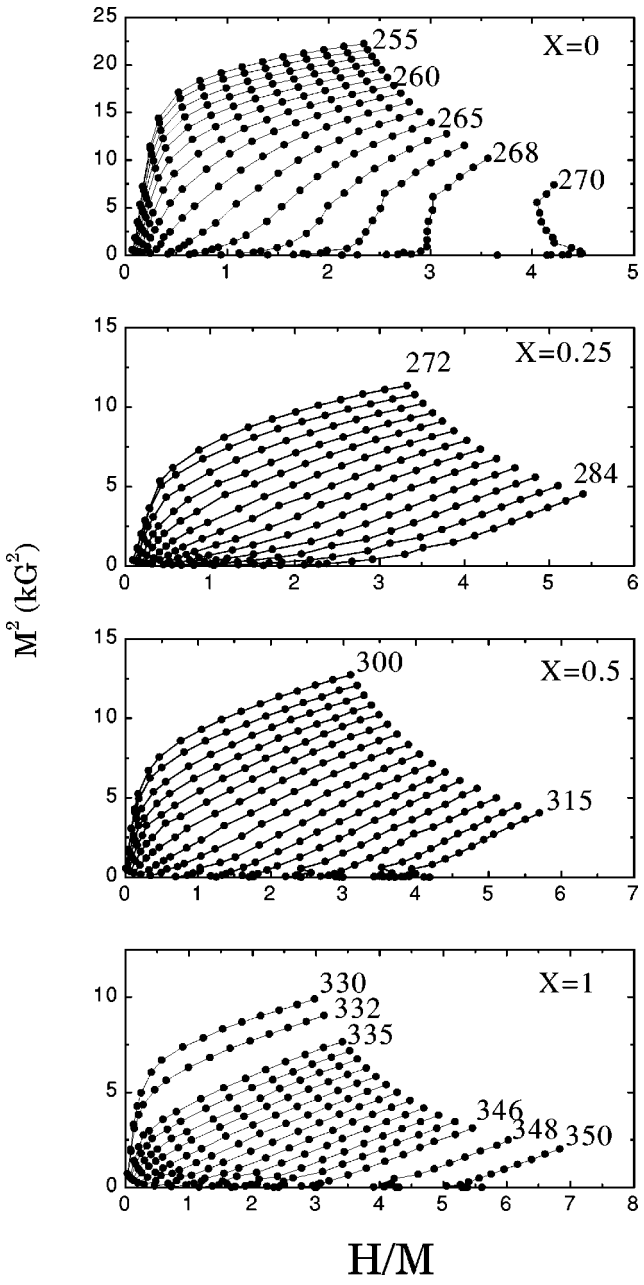

FIG. 2. Arrot plots (M^2 vs H/M) for selected $La_{0.67}(Ba_xCa_{1-x})_{0.33}MnO_3$ samples. The numbers indicate the temperatures of the isotherms in K.

So the M^2 vs H/M curves should be straight lines, the intercept of which on the H/M axis, determines the magnetic state (should be negative below T_c and positive above T_c). This mean-field approximation can be generalized to the so called modified Arrott-plots expression[34]

$$(H/M)^{1/\gamma}=C_1(T-T_c)+C_2M^{1/\beta} \tag{3}$$

which combines the relations for the spontaneous magnetization below T_c

$$M\sim(T_c-T)^{\beta} \tag{4}$$

and the inverse susceptibility above T_c

$$\chi^{-1}\sim(T-T_c)^{\gamma}. \tag{5}$$

According to Eq. (3) by an appropriate choice of β and γ the $(H/M)^{1/\gamma}$ vs $M^{1/\beta}$ plots should give parallel straight lines. Equation (2) is obtained for the mean field values $\beta=0.5$, $\gamma=1$. The critical exponents of the transition can be equivalently determined by scaling plots of the form $M/|t|^{\beta}=f_{\pm}(H/|t|^{\gamma+\beta})$ where $t=|T-T_c|$, $f_{\pm}$ is a scaling function and the plus or minus sign correspond to the ferromagnetic and paramagnetic regions, respectively.[35] By appropriate selection of the parameters T_c, β, and γ the data should collapse on two different branches for $T>T_c$ and $T<T_c$. In Fig. 2, M^2 vs H/M plots are shown for selected samples. It can be seen that for the samples with higher T_c the most of the data fall on straight lines in contrast with the $x=0$ sample where an anomalous behavior is observed. Usually, in bulk magnetization measurements, it is not possible to chose β and γ values that can make all the data fall on a straight lines because the low field data deviate from linearity and an extrapolation of higher field data is used.[36–38] Arrott plots are meaningful if the magnetic field is high enough so that possible domain or stray field effects are not significant and the macroscopically measured magnetization corresponds to the order parameter.[39] From the data presented in Fig. 2 it is obvious that the low field anomaly is much more pronounced in samples with lower T_c. However, even if we exclude several low field data points the change of slope of the curves around T_c still poses an ambiguity on the T_c determination. Since the slope is not constant along the curves we cannot find a set parameters β, γ that can make the set of $(H/M)^{1/\gamma}$ vs $M^{1/\beta}$ curves to be straight and parallel lines for a reasonable range of fields. In higher T_c samples, on the other hand, the situation is simpler. There is only one small region of low fields for which the curves deviate from linearity. The fact that for samples with $x\geqslant 0.25$ even simple M^2 vs H/M plots give straight lines signifies that the transition is conventional with exponents close to those of mean field theory. For the $x=1$ sample a T_c of 340 K can be calculated from the Arrott plots. Modified Arrott plots for parameters closer to those observed to other ferromagnetic materials ($\beta=0.32$–0.39, $\gamma=1.3$–1.4)[38] can give also straight lines but lower T_c values of 336–338 K. This ambiguity in the determination of β and γ values due to mutual dependence on the T_c parameter has been noted by Arrott[34] who found that the optimum choice of T_c falls linearly with $\delta=1+\gamma/\beta$ and proposed that Eq. (3) should be used to fit the actual M vs H data. This method provides a

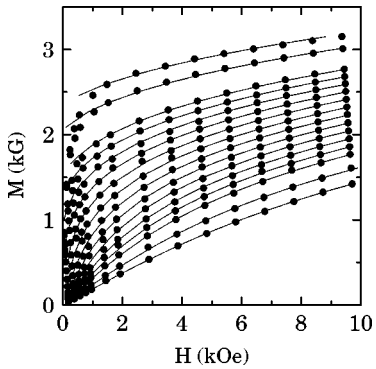

FIG. 3. M vs T data for the $x=1$ sample and theoretical curves derived from Eq. (3) for $\beta=0.464$, $\gamma=1.29$, $T_C=338.1$, $C_1=0.30$, and $C_2=0.39$ for the $La_{0.67}Ba_{0.33}MnO_3$ sample.

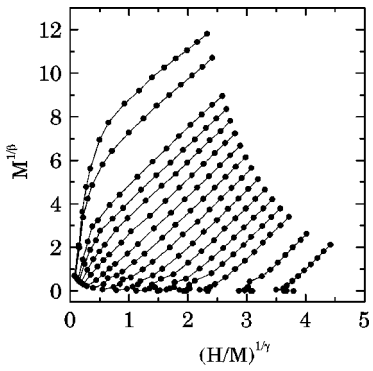

FIG. 4. Modified Arrott plot for the sample $La_{0.67}Ba_{0.33}MnO_3$ with $\beta=0.464$ and $\gamma=1.29$.

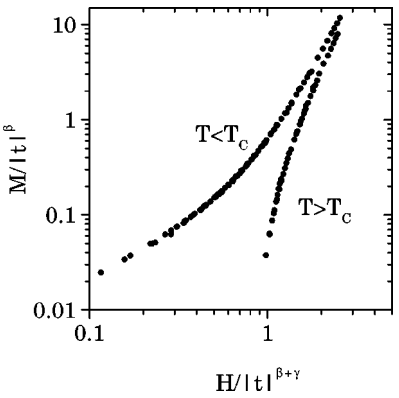

FIG. 5. Scaling plot $M/|t|^{\beta}$ vs $H/|t|^{\gamma+\beta}$ for the sample $La_{0.67}Ba_{0.33}MnO_3$ with $\beta=0.464$ and $\gamma=1.29$.

more quantitative way to find a best choice of β, γ, and T_c between values that would look equally good in scaling plots of the form $M/|t|^{\beta}=f_{\pm}(H/|t|^{\gamma+\beta})$. In Fig. 3 the M vs T data for the $x=1$ sample are shown along with theoretical curves derived from Eq. (3) for the parameters that give the best fit: $\beta=0.464(3)$, $\gamma=1.29(2)$, $T_c=338.1(2)$, $C_1=0.30(1)$, and $C_2=0.39(1)$. The numbers in the parentheses indicate the statistical errors of the last significant digit. Based on these parameters the modified Arrott plots (Fig. 4) and scaling plots (Fig. 5) can be constructed that prove the validity of the choice of β, γ, and T_c. Following the same method we calculated for the $x=1/2$ sample $\beta=0.402(3)$, $\gamma=1.11(2)$, $T_c=306.1(2)$, $C_1=0.40(1)$, and $C_2=0.22(1)$ and for the $x=1/4$ sample $\beta=0.356(4)$, $\gamma=1.12(3)$, $T_c=276.7(2)$, $C_1=0.42(3)$, and $C_2=0.14(1)$. The quality of the fit was equally good in the case of the $x=1/4$ and $x=1/2$ samples. The calculated values of the critical exponents are between those predicted for a three-dimensional (3D) Heisenberg model ($\beta=0.3$, $\gamma=1.4$, Ref. 35) and those predicted by mean field theory ($\beta=0.5$, $\gamma=1$).

V. CONCLUSIONS

In conclusion, in the $La_{0.67}(Ba_xCa_{1-x})_{0.33}MnO_3$ series, samples with $x\leqslant 0.4$ crystallize in the orthorhombic $Pnma$ structure, whereas samples with $x\geqslant 0.5$ in the rhombohedral $R\bar{3}c$ structure. As a result of structural changes due to Ca substitution by the larger Ba ions an increase of the transition temperature is observed. Only in samples with higher T_c ($x\geqslant 0.25$) the magnetic properties follow the expected behavior of a conventional second-order ferromagnetic transition. For these samples the values of critical exponents (β,γ) are between those predicted for a 3D Heisenberg model and those predicted by mean field theory.

[1] C. Zener, Phys. Rev. **81**, 440 (1951); **82**, 403 (1955).

[2] A. J. Millis, P. B. Littlewood, and B. I. Shraiman, Phys. Rev. Lett. **74**, 5144 (1995); A. J. Millis, B. I. Shraiman, and R. Mueller, *ibid.* **77**, 175 (1996).

[3] H. Röder, Jun Zang, and A. R. Bishop, Phys. Rev. Lett. **76**, 1356 (1996).

[4] J. J. Neumeier, M. F. Hundley, J. D. Thompson, and R. H. Heffner, Phys. Rev. B **52**, R7006 (1995).

[5] J. W. Lynn, R. W. Erwin, J. A. Bochers, Q. Huang, A. Santoro, J-L. Peng, and Z. Y. Li, Phys. Rev. Lett. **76**, 4046 (1996).

[6] R. H. Heffner, L. P. Le, M. F. Hundley, J. J. Neumeier, G. M. Luke, K. Kojima, B. Nachumi, Y. J. Uemura, D. E. MacLaughlin, and S-W. Cheong, Phys. Rev. Lett. **77**, 1869 (1996).

[7] J. M. De Teresa, M. R. Ibarra, P. A. Algarabel, C. Ritter, C. Marquina, J. Blasco, J. Garcia, A. del Moral, and Z. Arnold, Nature (London) **386**, 256 (1997).

[8] J. A. Fernandez-Baca, P. Dai, H. Y. Hwang, C. Kloc, and S-W. Cheong, Phys. Rev. Lett. **80**, 4012 (1998).

[9] R. Mahesh, R. Mahendiran, A. K. Raychauduri, and C. N. R. Rao, J. Solid State Chem. **120**, 204 (1995).

[10] H. Y. Hwang, S-W. Cheong, P. G. Radaelli, M. Marezio, and B. Batlogg, Phys. Rev. Lett. **75**, 914 (1995).

[11] J. M. D. Coey, M. Viret, L. Ranno, and K. Ounadjela, Phys. Rev. Lett. **75**, 3910 (1995).

[12] J. Fontcuberta, B. Martinez, A. Seffar, S. Pinol, J. L. Garcia-Munoz, and X. Obradors, Phys. Rev. Lett. **76**, 1122 (1996).

[13] J. Blasco, J. Garcia, J. M. De Teresa, M. R. Ibarra, P. A. Algarabel, and C. Marquina, J. Phys.: Condens. Matter **8**, 7427 (1996).

[14] A. Maignan, Ch. Simon, V. Caignaert, and B. Raveau, Z. Phys. B **99**, 305 (1996).

[15] P. G. Radaelli G. Iannone, M. Marezio, H. Y. Hwang, S-W. Cheong, J. D. Jorgensen, and D. N. Argyriou, Phys. Rev. B **56**, 8265 (1997).

[16] P. G. Radaelli, M. Marezio, H. Y. Hwang, and S-W. Cheong, J. Solid State Chem. **122**, 444 (1996).

[17] H. Kuwahara, Y. Moritomo, Y. Tomioka, A. Asamitsu, M. Kasai, and Y. Tokura, J. Appl. Phys. **81**, 4954 (1997).

[18] Y. Tomioka, H. Kuwahara, A. Asamitsu, M. Kasai, and Y. Tokura, Appl. Phys. Lett. **70**, 3609 (1997).

[19] A. Sundaresan, A. Magnain, and B. Raveau, Phys. Rev. B **56**, 5092 (1997).

[20] F. Millange, A. Maignan, V. Caignaert, C. Simon, and B. Raveau, Z. Phys. B **101**, 169 (1996).

[21] M. Medarde, J. Mesot, P. Lacorre, S. Rosenkranz, P. Fisher, and K. Gobrecht, Phys. Rev. B **52**, 9248 (1995).

[22] L. M. Rodriguez-Martinez and J. P. Attfield, Phys. Rev. B **54**, R15 622 (1996).

[23] N. Moutis, I. Panagiotopoulos, M. Pissas, and D. Niarchos (unpublished).

[24] F. Damay, C. Martin, A. Maignan, and B. Raveau, J. Appl. Phys. **82**, 6181 (1997).
[25] J. Fontcuberta, J. L. Garcia-Munoz, M. Suaaidi, B. Martinez, S. Pinol, and X. Obradors, J. Appl. Phys. **81**, 5481 (1997).
[26] P. Schiffer, A. P. Ramirez, W. Bao, and S. W. Cheong, Phys. Rev. Lett. **75**, 3336 (1995).
[27] R. D. Shannon, Acta Crystallogr., Sect. A: Cryst. Phys., Diffr., Theor. Gen. Crystallogr. **32**, 751 (1976).
[28] D. B. Wiles and R. A. Young, J. Appl. Crystallogr. **14**, 149 (1981).
[29] A. M Glazer, Acta Crystallogr., Sect. B: Struct. Crystallogr. Cryst. Chem. **28**, 3384 (1972); Acta Crystallogr., Sect. A: Cryst. Phys., Diffr., Theor. Gen. Crystallogr. **31**, 756 (1975).
[30] W. Archibald, J. S. Zhou, and J. B. Goodenough, Phys. Rev. B **53**, 14 445 (1996).
[31] A. Arrott, Phys. Rev. **108**, 1394 (1957).
[32] K. P. Belov, *Magnetic Transitions* (Boston Technical, Boston, 1965).
[33] P. G. De Gennes, Phys. Rev. **118**, 141 (1959).
[34] A. Arrott and J. E. Noakes, Phys. Rev. Lett. **19**, 786 (1967).
[35] H. E. Stanley, *Introduction to Phase Transitions and Critical Phenomena* (Clarendon, Oxford 1971).
[36] M. Seeger and H. Kronmuller, J. Magn. Magn. Mater. **78**, 393 (1989).
[37] Ch. V. Mohan, M. Seeger, and H. Kronmuller, J. Magn. Magn. Mater. **174**, 89 (1997).
[38] S. N. Kaul, J. Magn. Magn. Mater **53**, 5 (1985).
[39] A. Aharoni, J. Appl. Phys. **56**, 3479 (1984).